Static strength of gold compressed up to 127 GPa*

Jing Qiu-Min(敬秋民)†, Wu Qiang(吴 强), Liu Lei(柳 雷), Bi Yan(毕 延), Zhang Yi(张 毅), Liu Sheng-Gang(刘盛刚), and Xu Ji-An(徐济安)

Key Laboratory of Shock Wave and Detonation Physics, Institute of Fluid Physics, China Academy of Engineering Physics, Mianyang 621900, *China*

(Received 12 March 2012; revised manuscript received 25 April 2012)

Gold powder is compressed non-hydrostatically up to 127 GPa in a diamond anvil cell (DAC), and its angle dispersive X-ray diffraction patterns are recorded. The compressive strength of gold is investigated in a framework of the lattice strain theory by the line shift analysis. The result shows that the compressive strength of gold increases continuously with the pressure up to 106 GPa and reaches 2.8 GPa at the highest experimental pressure (127 GPa) achieved in our study. This result is in good agreement with our previous experimental result in a relevant pressure range. The compressive strength of gold may be the major source of the error in the equation-of-state measurement in various pressure environments.

Keywords: compressive strength, gold, diamond anvil cell, lattice strain theory

PACS: 62.20.fg, 62.50.–p, 07.35.+k **DOI:** 10.1088/1674-1056/21/10/106201

1. Introduction

The diamond anvil cell (DAC) combined with various fluid pressure media has become a typical assemblage to generate hydrostatic high pressures in the equation-of-state (EOS) measurements. However, an ideal hydrostatic environment cannot be sustained at above $\sim$ 15 GPa due to the solidification of all commonly used pressure media at room temperature.[1] Under such a condition, the stress in the pressure marker may not be consistent with the stress of the sample, if the strength of investigated sample differs from that of the pressure marker and/or both the sample and pressure marker do not yield under the non-hydrostatic compression.[2] When the pressure marker is harder than the sample, the pressure marker with higher incompressibility will give a slightly higher pressure due to stress concentration (or pressure intensification), while the softer one will give a lower value which is nearly close to the true pressure value of the sample.[3] For example, the maximum pressure difference between ruby (a kind of pressure marker) and a very soft sample can reach 12 GPa–18 GPa at 200 GPa.[4] Obviously, the pressure difference between a pressure marker and the investigated sample came from the presence of non-hydrostatic stress in a DAC device and has long been recognized to bias the EOS determinations.[5−7] To minimize pressure errors in EOS measurements, it is important to design the most effective combination of sample material and pressure standards, such as choosing an appropriate pressure marker to match the investigated sample in their strength and elastic properties.[8] In recent years, the yield strength and mechanical properties of many pressure markers were studied.[9−12] As one of the most widely used internal pressure markers in static high-pressure experiments, gold has attracted a great deal of attention.[13−17] Usually gold is used at pressures up to hundreds of pascals,[18,19] so it is desirable to extend the study on the yield strength of gold to more than 100 GPa. In this study we report on the yield strength of gold investigated at pressures up to 127 GPa in the framework of lattice strain theory by the line shift analysis. The result could provide data for designing a most effective combination of the sample and pressure markers to minimize pressure errors in EOS measurements.

2. Experimental detail

The modified Mao–Bell type DAC used for this experiment has a pair of beveled diamonds (the central flat of 150 μm and the culet size of 300 μm in di-

*Project supported by the Defense Industrial Technology Development Program (Grant No. B1520110001) and the Fund of Key Laboratory of Shock Wave and Detonation Physics of China (Grant No. 9140C6703031002).

†Corresponding author. E-mail: j_qm@163.com

© 2012 Chinese Physical Society and IOP Publishing Ltd

ameter, and a bevel angle of 7°). The T301 stainless steel gasket with an initial thickness of 250 μm was preindented to 25 GPa and a sample chamber with a diameter of 75 μm was drilled in the centre. The commercial polycrystalline gold powder (Alfa Aesar, USA, purity of 99.96%) with a typical average particle size of about 1 μm was contained in the sample chamber. In order to maximize the non-hydrostatic stress, the sample was compressed without any pressure transmitting medium. *In situ* high pressure angle-dispersive diffraction experiments were performed at the High-Pressure Station, 4W2 beamline at Beijing Synchrotron Radiation Facility (BSRF). The X-ray was monochromatized to 0.6199 Å (1 Å=0.1 nm). The beam size was focused to 15(H)×28(V) μm^2 by Kirkpatrick–Baez mirrors. The diffraction patterns were recorded on a Mar345 on-line image plate. All of the measurements were conducted at room temperature. The pressures were determined by the EOS of gold reported by Anderson *et al.*[20] to reduce the pressure error arising from the pressure gauge.

3. Method of data analysis

Compression of a solid without any fluid pressure medium in a DAC results in a non-hydrostatic stress state. The macroscopic stress in the sample is axially symmetric about the load axis of the DAC and leads to the shift of the diffraction lines. The difference between the axial and radial stress component (t) is taken as a measure of the compressive strength of the sample material.[21] For the sample with a cubic crystal structure, in the conventional DAC geometry the lattice parameter $a_m(hkl)$ calculated from the measured line positions $2\theta_{hkl}$ is given by the following relation:[22–24]

$$a_m(hkl) = M_0 + M_1[3(1 - 3\sin^2\theta_{hkl})\Gamma(hkl)], \quad (1)$$

with

$$\Gamma(hkl) = (h^2k^2 + k^2l^2 + l^2h^2)/(h^2 + k^2 + l^2)^2. \quad (2)$$

Here, M_0 and M_1 are constants at certain pressures. The plot of $a_m(hkl)$ versus $3(1 - 3\sin^2\theta_{hkl})\Gamma(hkl)$ (termed as the gamma-plot hereafter) is a straight line at certain pressures. The parameters M_0 and M_1 can be determined from such plots. The compressive strength t can be calculated from the relation,

$$t = -3M_1/\alpha M_0 S, \quad (3)$$

where S is the elastic anisotropy factor at a relevant pressure and obtained from the single-crystal elastic compliances S_{ij} as follows:

$$S = (S_{11} - S_{12} - S_{44}/2). \quad (4)$$

The details of this method are discussed in an earlier publication.[24] The term α determines the relative weight of the stress continuity (iso-stress model, Reuss limit[25]) and the strain continuity (iso-strain model, Voigt limit[26]). Some studies[27,28] suggested that the assumption of $\alpha = 1$ (iso-stress model) at high pressures is found to give satisfactory results. Thus, we took $\alpha = 1$ in the present study.

4. Results

The typical X-ray diffraction patterns are shown in Fig. 1. The four observed diffraction peaks from gold include (111), (200), (220), and (311). Above 83 GPa, the stars indicate the diffraction lines (100) and (110) of iron, which appear due to the deformation of gasket. Above 67 GPa, (311) reflection is off the range of the imagine plate detector and only (111), (200) and (220) reflections have been used to construct the gamma-plot according to Eq. (2). Typical gamma-plots at four different pressures are shown in Fig. 2. The experimental data are denoted by solid circles and the straight lines were obtained by the least-squares linear fitting. At each pressure, the parameters M_0 and M_1 can be determined from the corresponding straight line in the gamma-plot.

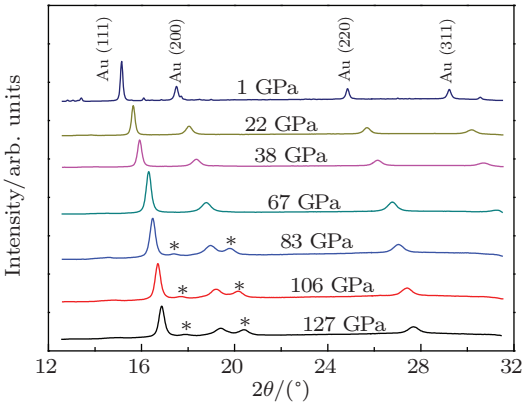


Fig. 1. (colour online) Typical angle dispersive X-ray diffraction patterns of gold at high pressures. All observed diffraction peaks (111), (200), (220), and (311) are labeled in the upper diffraction patterns. The stars indicate the diffraction lines (100) and (110) of iron.

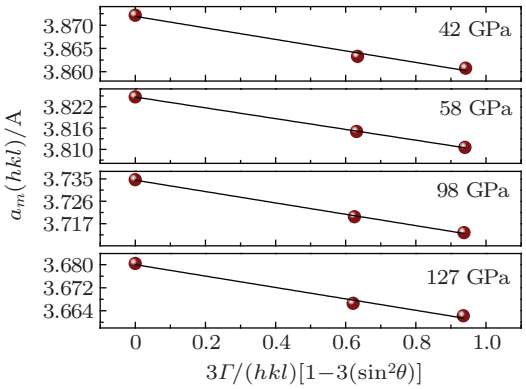


Fig. 2. (colour online) Typical determined lattice parameter $a_m(hkl)$ versus $3(1-3\sin 2\theta_{hkl})\Gamma(hkl)$ plots at four different pressures. The experimental data are denoted by solid circles and the straight lines are obtained by the least-squares linear fitting.

For calculating compressive strength t, the single-crystal elastic appliances must be known in advance. For gold, there are many reports[29,30] about its elastic constants and we can calculate S_{ij} by the following relations:

$$S_{11} = (C_{11} + C_{12})/(C_{11} - C_{12})/(C_{11} + 2C_{12}), \quad (5)$$

$$S_{12} = (-C_{12})/(C_{11} - C_{12})/(C_{11} + 2C_{12}), \quad (6)$$

$$S_{44} = 1/C_{44}. \quad (7)$$

To describe the pressure effect on elastic constants C_{ij}, the following form is adopted to determine C_{ij} at ultrahigh pressures (the subscript 0 means zero pressure value):[30]

$$C_{ij} = (C_{ij})_0 + (\mathrm{d}C_{ij}/\mathrm{d}P)_0 P(V/V_0)^{(1/3)}. \quad (8)$$

Dewaele and Loubeyre[30] have confirmed Eq. (8) by comparing the extrapolated C_{11}, C_{12}, C_{44}, and bulk modulus K with both experimental and theoretical data. We use Eq. (8) to extrapolate the elastic constants at pressures up to 127 GPa, and all parameters needed in Eq. (8) to calculate C_{ij} at high pressures are listed in Table 1 (cited from Ref. [29]).

Table 1. All parameters needed in Eq. (8) for calculating C_{ij} (cited from Ref. [29]).

$(C_{11})_0$/GPa	$(C_{12})_0$/GPa	$(C_{44})_0$/GPa	$(\mathrm{d}C_{11}/\mathrm{d}P)_0$	$(\mathrm{d}C_{12}/\mathrm{d}P)_0$	$(\mathrm{d}C_{44}/\mathrm{d}P)_0$
192.2	163.4	41.8	6.71	5.85	1.83

The compressive strength t of gold as a function of pressure is shown in Fig. 3. Approximately, we can find two regimes in the compressive strength of gold under pressures. It is obvious that t increases continuously with pressure increasing up to 106 GPa; and then increases with pressure but with a much smaller slope until the highest pressure (127 GPa in our experiment) is reached. Considering a somewhat large error in t above 106 GPa, the second regime is not so convinced. The change of slope at 106 GPa may be explained by material damage induced in highly strained specimen[31] or preferred orientation of the easily slip plane.[9,32] It is unclear which explanation holds for gold data and further experiments will be needed to resolve this point. The standard error of t arises from the least square fitting uncertainty of the $a_m(hkl)$ versus $3(1-3\sin^2\theta_{hkl})\Gamma(hkl)$ and the uncertainty of calculation of S according to Eqs. (2)–(8). In Fig. 3, only the error of t from the least square fitting uncertainty is shown.

The results determined by previous studies are also shown in Fig. 3 represented by different symbols for a comparison. Our results are in good agreement with earlier DAC data obtained using the conventional axial X-ray geometry[13] as well as other radial diffraction data.[14–16] It should be noted that the results in Ref. [16] were determined by the line width analysis method with the radial X-ray geometry. Our results show that though it is very soft under ambient conditions, the gold has a steady pressure hardening effect and its compressive strength has reached 2.8 GPa. Above 100-GPa pressure, it may become one of the major error sources in the equation-of-state measurements in non-hydrostatic pressure environments at ultra-high pressures when gold is used as an internal pressure marker.

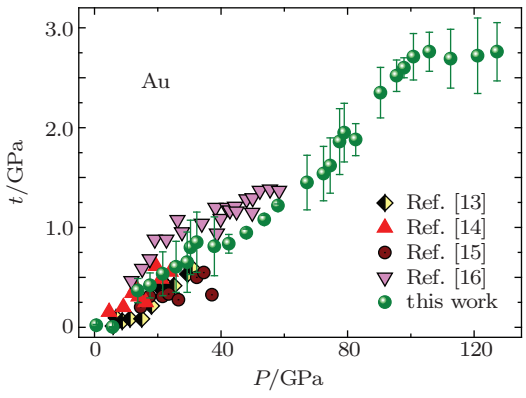


Fig. 3. (colour online) Pressure dependences of compressive strength derived from the lattice strain theory and data reported in earlier studies.

5. Conclusion

Gold powder is compressed under non-hydrostatic conditions up to 127 GPa in a DAC and the angle dispersive X-ray diffraction patterns are recorded. The gamma-plots at various high pressures are presented and the compressive strength of gold is determined from lattice strain theory. The result shows that the compressive strength of gold nearly continuously increases with the pressure increasing in an experimental pressure range. Above 100-GPa pressure, the compressive strength t reaches 2.8 GPa, which may be one of the major error sources in the equation-of-state measurements at ultra-high pressures when gold is used as an internal pressure marker.

Acknowledgement

The authors thank Dr. Chen Hai-Hua, Dr. Xiong Lun and Dr. Li Yan-Chun for experimental help. Experiments were conducted at 4W2 High-Pressure Station of BSRF, which is supported by Chinese Academy of Sciences (Grant Nos. KJCX2-SW-N03 and KJCX2-SW-N20).

References

[1] Miletich R, Allan D R and Kuhs W F 2000 *Rev. Mineral. Geochem.* **41** 447
[2] Wang J H and He D W 2008 *Acta Phys. Sin.* **57** 3397 (in Chinese)
[3] Sung C M Goetze C and Mao H K 1977 *Rev. Sci. Instr.* **48** 1386
[4] Meade C and Jeanloz R 1990 *Phys. Rev.* B **42** 2532
[5] Singh A K and Kennedy G C 1974 *J. Appl. Phys.* **45** 4686
[6] Kinsland G L and Bassett W A 1977 *J. Appl. Phys.* **48** 978
[7] Duffy T S, Mao H K and Hemley R J 1995 *Phys. Rev. Lett.* **74** 1371
[8] Conil N and Kavner A 2006 *J. Phys.: Condens. Matter* **18** S1039
[9] Weir S T, Akella J, Ruddle C, Goodwin T and Hsiung L 1998 *Phys. Rev.* B **58** 11258
[10] Jing Q M, Bi Y, Wu Q, Jing F Q, Wang Z G, Xu J A and Jiang S 2007 *Rev. Sci. Instr.* **78** 073906
[11] Kavner A and Duffy T S 2003 *Phys. Rev.* B **68** 144101
[12] Singh A K, Liermann H P, Akahama Y, Saxena S K and Menendez-Proupin E 2008 *J. Appl. Phys.* **103** 063524
[13] Meng Y, Weidner D J and Fei Y 1993 *Geophys. Res. Lett.* **20** 1147
[14] Duffy T S, Shen G Y, Heinz D L, Shu J F, Ma Y Z, Mao H K, Hemley R J and Singh A K 1999 *Phys. Rev.* B **60** 15063
[15] Duffy T S, Shen G Y, Shu J F, Mao H K, Hemley R J and Singh A K 1999 *J. Appl. Phys.* **86** 4729
[16] Singh A K, Liermann H P, Saxena S K, Mao H K and Usha Devi1 S 2006 *J. Phys.: Condens. Matter* **18** S969
[17] Wang J H, He D W and Duffy T S 2010 *J. Appl. Phys.* **108** 063521
[18] Akahama Y and Kawamura H 2002 *J. Appl. Phys.* **92** 5892
[19] Dewaele A, Loubeyre P and Mezouar M 2004 *Phys. Rev.* B **70** 094112
[20] Anderson O L, Isaak D G and Yamamoto S 1989 *J. Appl. Phys.* **65** 1534
[21] Ruoff A L 1975 *J. Appl. Phys.* **46** 1389
[22] Singh A K 1993 *J. Appl. Phys.* **73** 4278
[23] Singh A K, Balasingh C, Mao H K, Hemley R J and Shu J 1998 *J. Appl. Phys.* **83** 7567
[24] Singh A K and Takemura K 2001 *J. Appl. Phys.* **90** 3269
[25] Reuss A and Angew Z 1929 *Math. Mech.* **9** 49
[26] Voigt W 1910 *Lehrbuch der Kristalphysik* (Berlin: Teubner) p. 962
[27] Shieh S R and Duffy T S 2002 *Phys. Rev. Lett.* **89** 255507
[28] Merkel S, Wenk R H, Shu J, Shen G, Gillet P, Mao H K and Hemley R J 2002 *J. Geophys. Res.* **107** B11 2271
[29] Biswas S N, Klooster P Van't and Trappeniers N J 1981 *Physica* B **103** 235
[30] Dewaele A and Loubeyre P 2005 *Phys. Rev.* B **72** 134106
[31] Bridgman P W 1953 *J. Appl. Phys.* **24** 560
[32] Hu J B, Tan H, Yu Y Y, Dai C D and Ran X W 2008 *Chin. Phys.* B **17** 405